

addition, the contribution of π_2 in Q will be lower than 30%. These findings thus indicate that there is a strong case for revising the 60/90-min limit in respect to large jet airplanes.

Discussions

There is a high degree of conservatism built into the present airworthiness and operational codes in respect to modern jet airplanes. This is partially reflected in improved safety records. However, this unattended conservatism is penalizing for twin-jet airplanes in terms of operating economy and capability. In view of increasing fuel prices, overconservatism cannot be said to be very healthy.

A γ_m of 1.1%, although overconservative for modern jet airplanes, cannot be revised in isolation as it also affects the landing climb and balked landing requirements. A long-term view is necessary in the light of the new evidence. However, the 60/90-min rule can be easily revised.

The present 60/90-min ruling may act as a deterrent to the development of two-engine high-capacity jets like the B757 and B767 airbus, etc. While the present approach is to group turboprops, turbofans, and turbojets under the single head of turbine engines for the purpose of formulating airworthiness requirements, operational experience has established beyond doubt that jet engines are more reliable than turboprops. It may be worthwhile to treat turboprops and jet engines separately for this purpose and so enhance the operational capability and economy of jet airplanes.

Within the jet engine population, also, engine failure rates vary considerably with the type of engine. For the purpose of requirements like the 60/90-min one, each type of jet-engine airplane may be assessed on its own merit rather than assessing all types against a common rule.

References

- ¹Federal Aviation Regulations, Part 121, "Certification and Operations: Domestic, Flag, and Supplemental Air Carriers and Commercial Operators of Large Aircraft," Sept. 1980.
- ²"International Commercial Air Transport," Part I, ICAO Annex 6, Oct. 1972.
- ³U.K. Air Navigation Orders, 1974, Article 28.
- ⁴"Final Report of the Standing Committee on Performance," ICAO Document 7401-AIR/OPS/612, 1953, pp. 44-60.
- ⁵"The Derivation of Performance Standards for Jet Engine Aeroplanes," ARB Technical Note 5, 1957, p. 11.
- ⁶Le Guirriec, P., "Inflight Shutdown Rates for Jet Engines Comparative Analysis of the Shutdown Rates for the Main Jet Engines used by U.S. Airlines," Institut Du Transport Aerien (ITA) Bulletin 43, 1977, pp. 1015-1017.
- ⁷Le Guirriec, P., "Jet Engine—Inflight Shutdown Rates—Comparative Analysis of the Shutdown Rates for the Main Jet Engines used by United States Carriers in 1979," Institut Du Transport Aerien (ITA) Bulletin 39, 1980, pp. 929-931.

AIAA 82-4303

Laser Velocimeter for Large Wind Tunnels

Michael S. Reinath*
NASA Ames Research Center
Moffett Field, California

Introduction

THE measurement of velocity in large wind tunnels is normally performed using mechanical probes. This

Received May 17, 1982; revision received July 12, 1982. This paper is declared a work of the U.S. Government and therefore is in the public domain.

*Aerospace Engineer.

practice, although a basic, dependable method of making such measurements, can entail considerable complexity owing to the structure often required for probe support. Support structures can be bulky, complex, and costly, especially if probe translation is desired over long distances in a large wind tunnel test section.

The use of laser velocimetry for the flowfield measurements in large wind tunnels is far more desirable since it can be implemented with minimal mechanical complexity and with minimal modifications to the test section structure. By incorporating a variable-focus capability, a velocimeter can be used for surveying large regions within a wind tunnel test section without introducing objectionable support structures in the immediate vicinity of the model as would be required when mechanical probes are used. Accordingly, the velocimeter described herein is intended to be used in investigations that include V/STOL vehicle flowfield mapping for location and sizing of wakes and plumes,¹ wing-loading distribution determination without the need for pressure taps,² the aerodynamics of high-lift airfoils as well as rotating rotor blades,³ and vehicle wake studies.

The laser velocimeter described herein has been designed to fill the need for a long-range system that can operate in a large wind tunnel. The instrument has undergone preliminary testing and is now in the final stages of development. It is a single-color dual-beam backscatter system that is capable of sensing two orthogonal components of velocity. The system will be installed within the test section of the NASA Ames 40- \times 80-ft Wind Tunnel. Flow surveys will be accomplished through a combination of mechanical translation and rotation and optical focusing. A dedicated stand-alone microprocessor-based interface unit will be used for test-point position control, data acquisition, and display.

Velocimeter Description

An argon-ion laser capable of producing 9 W of continuous power at a wavelength of 514.5 nm is the source of laser light. A unique arrangement of two acousto-optic cells is used to accomplish beam splitting as well as frequency shifting (to eliminate flow direction ambiguity) functions. In this manner, a frequency difference between the two parallel output beams of 20 MHz is ultimately obtained. The optical system that focuses the beam pair to a particular point in the wind tunnel comprises three lens modules and a large folding mirror. The output lens module is a stationary singlet and has a clear aperture diameter of 33 cm; the intermediate module is also a stationary singlet element; and the module that first intercepts the parallel output beams is a movable triplet assembly. The folding mirror is 38 cm wide, 51 cm long, and 6.4 cm thick and is coated for 99.94% reflectance at the laser wavelength when the incidence angle is 45 deg.

A sketch of the installation and associated positioning hardware is shown in Fig. 1. Three scanning motions control the position of the velocimeter test point. The laser and optical components are mounted within a cylindrical aluminum housing 76 cm in diameter and 4.3 in length that can be rotated about its longitudinal axis (see Fig. 1) so that the test point can be positioned at any point along an arc of 45 deg to either side of the vertical. The package is mounted on linear bearings that attach to a rail support system to provide lateral positioning capability, and range control (optical focusing) is accomplished by translation of the movable lens module. Longitudinal positioning, on the other hand, is accomplished by repositioning the rail system, which is only temporarily attached to the tunnel floor. Each of the three scanning motions is made with a stepping motor through computer control; absolute optical shaft-angle encoders provide positive position readback.

A stand-alone microprocessor-based interface unit has been designed and fabricated in order to monitor encoder positions, provide motor control, and buffer the velocity

information during data acquisition. The unit has the additional capability of acquiring peripheral data on ten analog and four digital channels. Conditional sampling of the Doppler signal is possible based on signal level limit settings on four of the analog channels and on all of the digital channels. The upper and lower limits for conditional sampling are adjustable on the front panel of the interface unit. When the conditional mode is selected, no velocimeter signals are processed and transferred to memory unless each of the selected channels is within the preset limits.

The interface unit can be operated either manually from the front panel or may be slaved to a higher level computer through an IEEE 488 interface bus. Velocity values and test point position are displayed on the front panel in addition to the sampled values of selected analog and digital channels. Depending on data storage and graphics requirements, either a desktop computer with dual flexible disk mass storage or a high-speed mainframe minicomputer system with graphics capability can be used for remote data acquisition and control.

Velocimeter Capabilities

The scanning capabilities of the velocimeter permit measurements to be made over a large portion of the test section of the 40- \times 80-ft Wind Tunnel. The lateral motion of the optical package along the rail system covers a distance of 6 m with a positioning resolution of 0.025 cm. Ninety degrees of optical system rotation (± 45 deg from the vertical) is possible with a test point positioning resolution of 0.20 mrad, and the range adjustment is capable of scanning the test point from a distance of 2.6 m to a distance of 10 m, measured from the output lens, with a positioning resolution of 0.11 cm.

The spatial resolution of the velocimeter is limited to a greater degree by the length of the focal volume than by the mechanical positioning accuracy. At a range of 3 m from the output lens, the length of the focal volume is 0.33 cm (measured to the $1/e^2$ points); the length increases to 1.5 cm at a range of 10 m. The diameter of the focal volume is nearly at the diffraction limit over the intended range of operation and is approximately 0.025 cm at midrange.

The orthogonal velocity components sensed by the velocimeter are indicated in Fig. 2. The accuracy of the velocity measurement is influenced by 1) the clock speed of the counter-type signal processor, 2) the magnitude of the Doppler frequency, and 3) the number of cycles chosen per Doppler burst. For example, at a range of 6.5 m, with a signal frequency of 20 MHz, and 16 cycles used for processing, an accuracy of ± 0.3 m/s can be expected (neglecting statistical and systematic uncertainties). The accuracy can be improved by frequency downmixing; for example, if the 20-MHz signal

is downmixed to 10 MHz, the expected velocity uncertainty is reduced to ± 0.07 m/s, assuming other parameters remain unchanged.

In its present configuration, the velocimeter does not measure both orthogonal components of velocity simultaneously (see Fig. 2). Instead, the desired component is selected by using a novel parallel-beam rotation device that rotates the output beam pair by 90 deg before it enters the lens system. The third velocity component can be obtained indirectly by measuring the velocity components at the same point in the flowfield from two different lateral locations and by transforming these measured components to a common orthogonal coordinate system oriented with respect to the wind

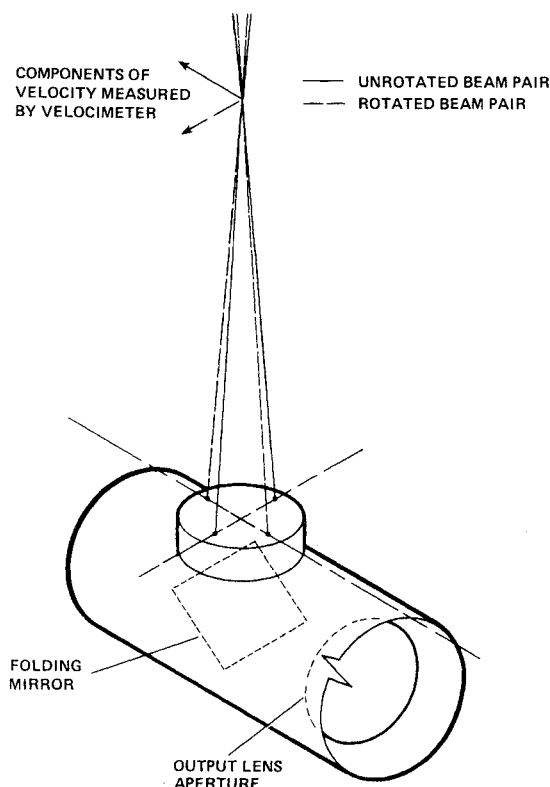


Fig. 2 Front section of velocimeter showing beam pair rotation feature and the corresponding velocity components.

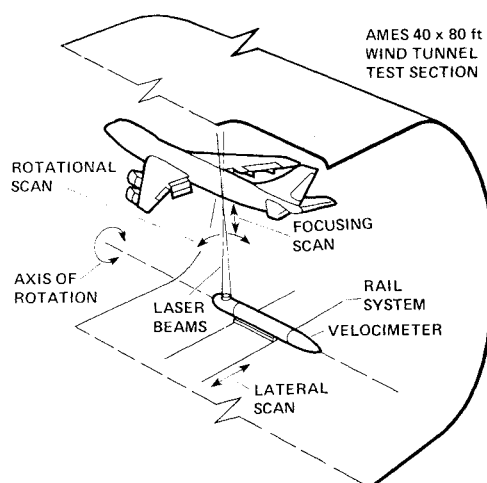


Fig. 1 Velocimeter installation in the Ames 40- \times 80-ft Wind Tunnel showing test-point positioning features.

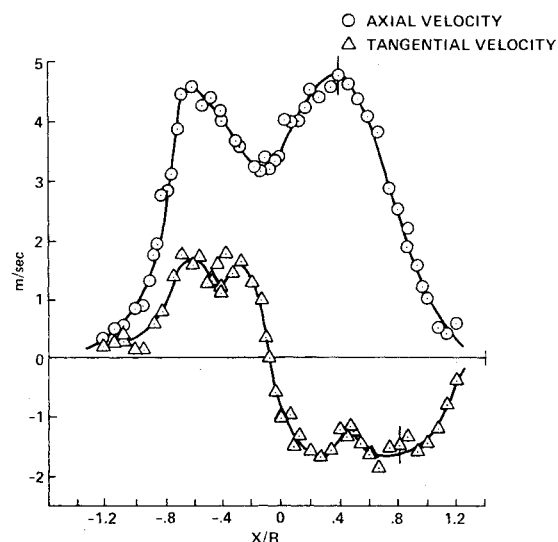


Fig. 3 Velocity distribution across air circulation fan; X is measured along survey line with origin at axis of symmetry; R is the fan radius (37.8 cm).

tunnel. The accuracy of the velocity components determined by this method depends on 1) the coupling angle determined by the two lateral locations of the velocimeter, 2) the statistical uncertainty due to sampling, and 3) systematic uncertainties resulting from positioning and calibration errors.⁴ The effect of these uncertainties on the ultimate measurement accuracy is currently being studied.

Preliminary Velocimeter Evaluation

A limited flow survey of the flow generated by a two-bladed, 0.76-m-diam, industrial-type air circulation fan was conducted in order to evaluate system performance. The survey was made across the fan face parallel to the plane of rotation and through the axis of symmetry at a distance of 0.56 fan diameters from the fan on the downstream side. The fan rotated in a clockwise direction when viewed from the downstream side.

The data presented in Fig. 3 were obtained while operating the velocimeter at a range of 6.4 m and a laser output power of 2.5 W. A light aerosol of mineral oil seeding was introduced on the upstream side of the fan to reduce data acquisition time; however, excellent signals were also obtained with the natural seeding present in the area of the fan. A desktop computer and a counter-type signal processor were used for data acquisition and reduction. Seventy velocity samples were acquired per data point; a 95% confidence interval for 70 samples is shown in Fig. 3.

A slight asymmetry of the velocity profile is apparent from Fig. 3. This behavior was caused by the influence of a wall located at a distance of two fan diameters from and parallel to the axis of symmetry.

It is interesting to note that a velocity shear of 41 (m/s)/m near the fan center was resolved from a range of 6.4 m. This shear does not necessarily represent the limit of resolution of the velocimeter since the test flow was selected primarily for reasons of convenience and was not intended to be used to determine the limiting performance of the velocimeter.

Velocimeter Applications

In its current configuration, the velocimeter is designed for use in the Ames 40- \times 80-ft Wind Tunnel. However, it should be emphasized that the basic design does not preclude use of the system in the Ames 80- \times 120-ft Wind Tunnel or at the Ames Outdoor Aerodynamic Research Facility. To operate in these other facilities, it is necessary to extend the range capability to 20 m, and a replacement output lens system has been designed and fabricated to meet this requirement. To accept these lenses the velocimeter requires minor modifications, and a test at the longer range has not yet been performed.

The first use of the velocimeter is planned for Dec. 1982 at which time it will be used to make a flow quality survey in the Ames 40- \times 80-ft Wind Tunnel.

References

- 1Zalay, A.D., Brashears, M.R., Jordan, A.J., Shrider, K.R., and Vought, C.D., "Measurement of a Flow Around V/STOL Aircraft with an LDV System," *Journal of Aircraft*, Vol. 17, Dec. 1980, pp. 835-836.
- 2Orloff, K.L., "Spanwise Lift Distribution on a Wing from Flowfield Velocity Surveys," *Journal of Aircraft*, Vol. 17, Dec. 1980, pp. 875-882.
- 3Biggers, J.C. and Orloff, K.L., "Laser Velocimeter Measurements of the Helicopter Rotor-Induced Flowfield," *Journal of the American Helicopter Society*, Vol. 20, Jan. 1975, pp. 2-10.
- 4Orloff, K.L. and Snyder, P.K., "Laser Doppler Anemometer Measurements Using Nonorthogonal Velocity Components: Error Estimates," *Applied Optics Journal*, Vol. 21, Jan. 1982, pp. 339-344.

AIAA 82-4304

Helicopter Rotor Performance Evaluation Using Oscillatory Airfoil Data

V.S. Holla*

Indian Institute of Science, Bangalore, India
and

A.R. Manjunath† and J. Nagabhushanam†
Hindustan Aeronautics Ltd., Bangalore, India

Introduction

IN helicopter design, the accurate evaluation of the rotor performance is an important step for an efficient design of the rotor. From an aerodynamic point of view the performance of the rotor depends mainly on the sectional aerodynamic properties of the blades, under steady and unsteady flow conditions. Under certain conditions, such as in hover or in flight with low forward velocity, two-dimensional steady-state sectional data may be quite sufficient, but at high forward speeds with the blade experiencing flapping and pitching oscillations, it becomes quite essential to use the unsteady aerodynamic data to get not too conservative estimates of the rotor performance. Nagabhushanam^{1,2} has developed a blade response program for the case of forward flight. In that program, two-dimensional steady-state aerodynamic data were used to get the response characteristics, thus giving a conservative estimate of blade response. Hence it is quite necessary to use the unsteady aerodynamic data in the Nagabhushanam program to get a realistic picture. The results of such a calculation as compared with those obtained by Nagabhushanam are presented in this Note.

Theoretical Analysis

The generalized differential equation for the blade response is given by

$$\frac{\partial^2}{\partial x^2} \left(EI \frac{\partial w^2}{\partial x^2} \right) - \frac{\partial}{\partial x} \left(N(x) \frac{w}{x} \right) + m(x) \frac{\partial^2 w}{\partial t^2} = T(x, t) \quad (1a)$$

where $T(x, t)$ is the external force, i.e., the aerodynamic force, acting on the blade. The deflection $w(x, t)$ and the aerodynamic load $T(x, t)$ are interdependent and in general it is difficult to get a closed-form solution for $w(x, t)$. Using generalized coordinates the deflection $w(x, t)$ is expressed as

$$w(x, t) = \sum_{i=1}^m Q_i(t) f_i(x) \quad (1b)$$

where $Q_i(t)$ is the general coordinate, $f_i(x)$ is the i th natural mode shape, and m is the number of modes considered.

Because of the orthogonal property of the mode shapes, the left-hand side of Eq. (1a) for any mode becomes independent of the other modes, but the aerodynamic load $T(x, t)$ contains contributions from all modes and hence Eq. (1a) cannot be solved independently for each mode. The numerical procedure developed for solving Eq. (1a) is explained in Appendix I of Ref. 1.

Received Dec. 1, 1981; revision received July 22, 1982. Copyright © American Institute of Aeronautics and Astronautics, Inc., 1982. All rights reserved.

*Assistant Professor, Aerospace Engineering Department.

†Design Engineer.